



Published in final edited form as:

Neuroimage. 2015 July 15; 115: 191–201. doi:10.1016/j.neuroimage.2015.04.048.

Axon diameter and axonal transport: *In vivo* and *in vitro* effects of androgens

M Pesaresi¹, R Soon-Shiong¹, L French¹, DR Kaplan², FD Miller², and T. Paus¹

¹Rotman Research Institute, University of Toronto, 3560 Bathurst Street, Toronto, Ontario, M6A2E1, Canada

²Program in Neuroscience and Mental Health, Hospital for Sick Children, Toronto, Ontario, Canada

Abstract

Testosterone is a sex hormone involved in brain maturation via multiple molecular mechanisms. Previous human studies described age-related changes in the overall volume and morphological properties of white matter during male puberty. Based on this work, we have proposed that testosterone may induce an increase of radial growth and, possibly, modulate axonal transport. In order to determine whether this is the case we have used two different experimental approaches. With electron microscopy, we have evaluated sex differences in the structural properties of axons in the corpus callosum (splenium) of young rats, and tested consequences of castration carried out after weaning. Then we examined *in vitro* the effect of the non-aromatizable androgen Mibolerone on the structure and bidirectional transport of wheat-germ agglutinin vesicles in the axons of cultured sympathetic neurons. With electron microscopy, we found robust sex differences in axonal diameter (males>females) and g ratio (males>females). Removal of endogenous testosterone by castration was associated with lower axon diameter and lower g ratio in castrated (vs. intact) males. *In vitro*, Mibolerone influenced the axonal transport in a time- and dose-dependent manner, and increased the axon caliber as compared with vehicle-treated neurons. These findings are consistent with the role of testosterone in shaping the axon by regulating its radial growth, as predicted by the initial human studies.

Keywords

axon; myelin; testosterone; axon transport; white matter

© 2015 Published by Elsevier Inc.

Corresponding author: Tomáš Paus, Rotman Research Institute, 3560 Bathurst St., Toronto, Ontario, Canada, M6A 2E1; tpaus@research.baycrest.org; Phone: 001-416-785-2500 x 3505; Fax: 001-416-785-4230.

Conflict of interest: The authors do not have any conflict of interest related to the reported work.

Publisher's Disclaimer: This is a PDF file of an unedited manuscript that has been accepted for publication. As a service to our customers we are providing this early version of the manuscript. The manuscript will undergo copyediting, typesetting, and review of the resulting proof before it is published in its final citable form. Please note that during the production process errors may be discovered which could affect the content, and all legal disclaimers that apply to the journal pertain.

Introduction

Maturation of white matter (WM) is a complex process involving changes in axonal diameter and myelin thickness, with progressive fine-tuning of the structure and function of the axon-myelin system (Ullén, 2009). Previous studies in our laboratory showed a positive correlation between testosterone levels and WM volume in adolescent males with the more efficient form of androgen receptor (AR). Furthermore, indirect evidence suggests that testosterone may influence WM volume in male adolescents by increasing axon diameter and not myelination (Perrin et al., 2009).

Axons are the main constituents of WM, occupying almost 90% of its total volume (Wang et al., 2008). Axons come in different sizes: some are thin, others thick, and different sizes are often mixed within the same fascicle (Peters et al., 1991). In myelinated axons, the ratio between axon diameter and fiber (axon + myelin thickness) diameter – the so-called *g* ratio – appears to increase as a function of axon diameter, indicating a relatively thinner myelin sheath in large axons (Berthold et al., 1983; Chatzopoulou et al., 2008; Gillespie and Stein, 1983). Distribution of axon diameter might relate to the heterogeneity of information transfer of a nerve bundle or fascicle (Perge et al., 2012). Besides the classical function as conductors of action potentials, axons also provide a physical conduit for the transport of a wide variety of cargos to the synapse. Thus, the axonal transport is a fundamental process to form the cellular networks of the nervous system and ensure a proper flow of information throughout the brain (reviewed in Paus et al. 2014). The key molecules for the microtubule-based axonal transport are motor proteins, members of the kinesins and cytoplasmic dynein superfamilies. Kinesins transport a cargo anterogradely toward the synapse, while dyneins move it retrogradely towards the cell body (Hirokawa et al., 2010). Maintenance of neuronal homeostasis depends on the fine regulation of motor proteins and cytoskeleton components engaged in the axon transport (Colin et al., 2008; Morfini et al., 2002; Perrot and Julien, 2009). Cytoskeletal elements have a dual role in the regulation of axon transport: they form the “tracks” along which the cargos are transported, and they are responsible for radial growth of the axon (Barry et al., 2010). In the context of the work described here, it is of interest that there is a reciprocal influence of the axonal radial growth on the axon transport and of the effect of the axon transport on axonal radial growth. On one hand thicker axons may accommodate a higher rate of axonal transport (Murayama et al., 2006). On the other hand, transport of cytoskeleton elements (containing tubulin and neurofilament proteins) plays an important role in regulating the axon diameter (Eyer and Peterson, 1994; Xia et al., 2003). As such, modulation of microtubule-based axonal transport under the influence of sex steroids during puberty and adolescence might affect the axon diameter and their distribution and, in turn, the performance of various WM pathways in a sex-dimorphic way.

Although the role of androgens in brain reorganization during the pubertal period has been recognized (Durdiakova et al., 2011; Herting et al., 2012; Peper et al., 2011), the exact mechanism of their action and how these differences are sustained at the microstructural level remain poorly understood. We have hypothesized that testosterone influences processes that determine axonal diameter and, in doing so, the macroscopic properties of WM assessed *in vivo* with MRI (Perrin et al. 2009, Paus and Toro 2009). Here we test this hypothesis using two experimental approaches. First we use electron microscopy to assess

the effect of testosterone on axon morphology in the splenium of the corpus callosum of young male and female rats, and after real or sham castration (after weaning) of male (adult) rats. We have chosen the callosal splenium (posterior fifth) as a model system because this structure has been the subject of previous research on sexual dimorphism (Kim et al. 1996; Kim and Juraska 1997). Second, due to the close relationship between axon transport and axon radial growth, we evaluated the effects of androgens on axonal transport by quantifying the movement of wheat-germ agglutinin (WGA) vesicles in the axons of cultured sympathetic neurons treated with Mibolerone, a non-aromatizable synthetic androgen. Our results are consistent with the possibility that testosterone plays a key role in the pubertal maturation of WM pathways by modulating the cellular processes that affect the dynamic turnover of cytoskeletal matrix responsible for the axonal structure.

Materials and Methods

Animals

Experimental animals were young (70 post-natal days) male and female wild-type Wistar rats, ordered from Charles River (St. Constant, Quebec, Canada). Rats were assigned to the following experimental groups: Experiment 1 (6 intact males, M; and 6 intact females, F); and Experiment 2 (10 sham castrated M; 10 sham castrated F; and 10 castrated males, M gx). Real or sham castrations were done at pre-pubertal stage (21 post-natal days) at Charles River; rats were shipped on post-natal day 65.

Five days after delivery (70 days of age), rats were weighed, deeply anesthetized with isoflurane and perfused through the left cardiac ventricle with 0.9% NaCl at 37°C, followed without interruption by 1% freshly prepared para-formaldehyde and 1% glutaraldehyde in 0.1M phosphate buffer at 37°C. After perfusion, the brain was removed and a slice (200 µm thick) of the medial section of the right hemisphere was taken, exposing the corpus callosum (CC) in plain view. The splenium was removed and prepared for electron microscopy. Briefly, tissues were postfixed in osmium tetroxide, dehydrated through ethanol to propylene oxide and embedded in Spurr's resin. Blocks containing the tissue samples were cut at 60 nm using an Ultracut E ultramicrotome (Leica, Nussloch, Germany) and collected on a 200-mesh grid (Agar Scientific, Stansted, UK). These sections were stained in 3% uranyl acetate and 1% lead citrate before proceeding with electron microscopy carried out on a Hitachi (Tokyo, Japan) H-600 transmission electron microscope operated at 75 kV.

Morphometric Analysis

To investigate the entire area of the splenium, one micrograph was taken at 10,000x magnification from eight different areas along the dorsal-to-ventral extent of the splenium in each rat; the sampled region did not include the hippocampal commissure (Figure 1A). For myelinated axons, diameter was calculated as follows. Using ImageJ software (<http://rsb.info.nih.gov/ij/>), the micrographs were transformed into binary images: the axon appeared white and myelin black. Next, we used the wand (tracing) tool to select thresholded pixels forming a contiguous area: we selected first a single pixel within an axon and then expanded this selection to all adjacent (white) pixels bound by the encircling myelin. The cross-sectional area of these pixels (i.e., the axon area) was measured

automatically. In this manner, we calculated the cross-sectional area of about 1,000 myelinated axons in each rat. The g ratio, the ratio between the axon diameter and fiber diameter (axon diameter + myelin sheath), was estimated by measuring the minimum and maximum axon diameter and the minimum and maximum fiber diameter of each axon using the same ImageJ software; the g ratio was obtained by dividing the mean axon diameter by the mean fiber diameter. The g ratio was calculated in about 400 myelinated axons for each animal in Experiment 1 and in a subset of animals (n=5 per group) in Experiment 2. Axon diameter, estimated as the mean of the minimum and maximum axon diameter, was also measured about 50 unmyelinated axons in each rat in a subset of animals (n=5 per group) in Experiment 2. Only axons with regular shape were measured. The distribution of axons was analyzed for each animal and the skewness was calculated as follows: $\frac{\sum (x-\mu)^3}{(N-1)\sigma^3}$, where \sum means sum all the values, μ represents a sample mean and σ is the sample standard deviation. The rater was blind to the sex and castration status of the axons under examination.

Western blot analysis

We measured concentrations of AR protein in the fresh superior thoracic ganglion and cerebral cortex from adult rats, as well in the sympathetic cell culture from P5 rats using Western blotting as described previously (Vaillant et al., 1999). We used a rabbit polyclonal AR antibody, PG-21 (1:200; Upstate Biotechnology, NY, USA). Protein bands were visualized with a goat anti-rabbit horseradish peroxidase-conjugated secondary antibody (1:10000; Sigma, ON, Canada).

Immunocytochemistry

To determine the AR distribution in the cells, we performed immunohistochemistry on sympathetic cell cultures. Immunocytochemistry was performed as described previously (Vaillant et al., 2002). We used PG-21 (1:20) and a goat anti-mouse Alexa 488 (Life Technologies, Inc., ON, Canada) as the primary and secondary antibodies, respectively.

Axonal Transport: Primary neuron cultures

To determine whether testosterone affects axonal transport, we analyzed time-lapse imaging of fluorescent WGA vesicles in axons of cultured neurons from the superior cervical ganglia of neonatal rats (PN 5). This culture system was previously used to analyze both fast and slow axonal transport (Schwab et al., 1979; Wang and Brown, 2001, 2002). Sympathetic neuron cultures were prepared as described previously (Vaillant et al., 1999). Briefly, sympathetic neurons were dissected from superior cervical ganglia (SCG) of rat pups (postnatal days 3 to 5) supplied by Charles River Canada. Media used were supplemented with 2 mM L-glutamine (Cambrex, MD, USA) and 100 μ g/ml penicillin/streptomycin (Cambrex). On Day 1, neurons were plated on collagen-coated 8-chamber cover slip (Nalge Nunc, NY, USA) at a density of 0.4 ganglia/well in Ultraculture medium (Cambrex) including 3% fetal bovine serum (FBS; Cambrex), 0.7 mM cytosine arabinoside (Sigma, ON, Canada) and 25 ng/ml nerve growth factor (NGF; CedarLane, ON, Canada). Neurons were plated in a corner of the well so that axons could be traced from the cell body to the growth cone, thus allowing us to determine the orientation of the axons in the time-lapse movies. On Day 3, the medium was changed to Ultraculture (w/o serum) including 20 ng/ml

NGF, 0.4 µg/ml WGA Alexa-546-conjugated (Invitrogen-Molecular Probes, ON, Canada), and either Mibolerone, (Toronto Research Chemicals, ON, Canada) at concentration of 4nM (4M) or 10nM (10M) or ethanol vehicle control (Ctrl). On the same day, to observe the movement of vesicles following WGA internalization, cells were transferred to a 37°C air-heated stage on spinning disk confocal microscopy (Yokogawa, Japan) equipped with an x63 oil-immersion objective. WGA- Alexa-546-conjugated-vesicles were observed by using a fluoresceinisothio-cyanate (FITC) filter set. Consecutive confocal images were collected at a rate of 10 frames/sec. The data were collected for each condition at three different time points (06hrs, 24hr, 48hrs after application of WGA and Mibolerone/Vehicle).

Axonal Transport: Image Processing and Analysis

Data were collected from 20 tissues, each derived from a different litter. Each tissue was used for 360 “experiments” (wells) divided evenly across the three conditions (4M Mibolerone, 10M Mibolerone, Vehicle). An WGA-vesicle was considered mobile if it moved between two consecutive frames at a velocity > 0.1 µm/s. Motion analysis was performed by tracking the position of the vesicle in successive time-lapse image frames using Image-Pro 3D analyzer 7.0 software (Media Cybernetics, Inc). The rater was blind to the experimental conditions. Vesicle tracking data were grouped into periods of forward-moving and not-forward-moving movements (i.e., pauses). For each period of forward movement, distance (run length) and duration were calculated. To calculate an average velocity per vesicle (in µm/s), we divided the forward-run length by its duration. For each vesicle, we also calculated the percent time spent moving (In Motion%): duration of movement/duration of measurement X 100. In addition, we quantified peak velocity, maximum run-length and the ratio of anterograde to retrograde movement (Antero/Retro). Vesicle based statistics were tabulated automatically.

Axon diameter in primary neuron cultures

Axon diameter was evaluated in a subset of experiments derived from seven litters. For the analysis of axon diameter, control and Mibolerone-treated cells were fixed overnight in 2% formaldehyde, 0.1% glutaraldehyde. The next day, cells were prepared for the electron microscopy as described above. Axon diameter was calculated from micrographs taken at 20,000x magnification, using automatic analyses of the cross-sectional area as previously described. The axon diameter was calculated in about 2,000 axons in each condition. Since axons and dendrites are difficult to distinguish in cell cultures, only spatially isolated regions, far from the corner where neurons were plated were selected for observation. This minimized measurements of ambiguous neuronal processes. The rater was blind to the experimental conditions.

Statistical analyses

The data were analysed using JMP software (SAS Institute Inc). Standard methods were used to obtain summary statistics. Differences among groups were assessed by ANOVA or Student’s t test for continuous parameters, chi-square test for categorical parameters. The median values for axonal diameter and g ratio as well as the mean values of skewness from M, F and M gx were compared using 1-way ANOVAs followed by Student’s t-tests (Bonferroni corrected for multiple comparisons). Logistic regression was used to assess the

contribution of treatment and time for the prediction of directionality of vesicles movements. For all analyses, $p < 0.05$ (corrected) was considered significant.

Cohen's d was also calculated as an indicator of effect size (the mean difference divided by the mean SD).

Results

I. Effect of testosterone on axon morphology in the splenium of young male and female rats

Animal body weight—As expected, body weight was higher in males than in females in both experiments (Experiment 1: M, 380.3 ± 5.2 g; F, 235 ± 6.4 g; $n=6$ per group; $p=0.001$); castrated males weighed less than intact males but more than females (Experiment 2: M, 396 ± 6.6 g; F, 240 ± 7.4 g; M gx 358 ± 5.7 g; $n=10$ per group; M vs. F, $p=0.001$; M vs. M gx, $p=0.01$; M gx vs. F, $p=0.001$).

Axon diameter and g ratio—In Experiment 1, we observed sex differences in myelinated axon diameter, with males having larger axons than females (M, 529 ± 31.71 ; F, 456 ± 19.71 ; $n=6$ per group; $p=0.001$, percent difference = 14.82%, Cohen's d effect size = 2.8; Figure 1C). This sex difference was confirmed in Experiment 2 (sham castrated male, M, 563 ± 41.84 ; sham castrated females, F, 469 ± 27.37 ; $n=10$ per group; $p=0.001$, percent difference = 18.22%, $d=2.7$; Figure 2A [M, F]). Furthermore, in Experiment 2, we observed that castration (after weaning) was associated with smaller axon diameter (in young adulthood), as compared with intact males (M, 563 ± 41.84 ; M gx, 502 ± 21.24 ; $n=10$ per group; $p=0.001$, percent difference = 11.46%, $d=1.84$; Figure 2A) but did not differ from intact females (F, 469 ± 27.37 ; M gx, 502 ± 21.24 ; $n=10$ per group; $p=0.069$; Figure 2A). In contrast to myelinated axons, there were no sex differences in the diameter of unmyelinated axons (M, 229 ± 23.90 ; F 249 ± 17.74 ; M gx, 502 ± 21.24 ; $n=5$ per group; $p=0.5$).

In addition to axon diameter, we evaluated g ratio in a subset of rats. In both Experiment 1 and 2, g ratio was higher in males compared with females. Castrated males had lower g ratio than intact males but did not differ from intact females (Experiment 1: M, 0.77 ± 0.01 ; F, 0.74 ± 0.02 , $n=6$ per group, $p=0.02$, percent difference = 3.97%, $d=1.89$; Experiment 2: M, 0.81 ± 0.02 ; F, 0.75 ± 0.02 ; M gx 0.77 ± 0.02 ; $n=5$ per group; M vs. F, $p=0.004$, percent difference = 7.69%, $d=3.6$; M vs. M gx $p=0.0195$, percent difference = 5.06%, $d=2.0$; M gx vs. F, $p=0.209$; Figures. 1D and 2B). Lastly, we plotted individual observations from both experiments to depict the relationship between axon diameter and g ratio (Figure 2C and D). The non-linear relationship between the two measures is demonstrated by the locally weighted scatterplot smoothing curves (LOESS). As expected, in both Experiment 1 and 2, g ratio increases as a function of axon diameter. Comparing males with both females and M gx shows divergence in the average g ratio for axons with diameters in the range of 400–800 nm. For statistical purposes, however, only Figures 2A and 2B should be considered as these represent group averages of g ratios (medians), with each median being based on about 400 myelinated axons per rat.

Axon diameter distribution—We then tested for the presence of sex differences in the distribution of axons with various diameters. For each group of rats, we characterized the distribution of axon diameter using the skewness $((\text{diameter}-m)/SD)^3$, a measure of the asymmetry of a distribution. Figure 3 provides an overview of the axon-diameter distributions in the two experiments. In both Experiment 1 and 2, the axon distribution of intact males spans a fairly broad range, with a positive skew toward larger diameter (Experiment 1: M skewness 1.34; Experiment 2: M skewness 1.36). In females, on the other hand, axon distribution was narrower and fairly symmetrical, with a smaller skew toward larger axons (Experiment 1: F skewness 0.72; Experiment 2: F skewness 0.58). Interestingly, in castrated males, axon distribution was nearly identical to that observed in intact females; it was narrow and fairly symmetrical, with a small skew (skewness of 0.55).

II. Effects of synthetic testosterone, Mibolerone, on axonal transport in primary neuron culture

Expression of AR in sympathetic neurons—The presence of AR was evaluated on the total proteins extracted from superior cervical ganglion and sympathetic cell culture. Cerebral cortex of the rat was used as positive control (DonCarlos et al. 2006). Figure 4A shows results of the Western blots performed using the PG-21 antibody recognizing the first 21 amino acids of the human AR. Immunoreactive bands with a molecular weight close to 110 kDa, as expected for the AR protein (Sato et al., 1997), were present in all homogenates. A doublet was observed in lysates from SCG and sympathetic neurons (sy) reflecting the phosphorylated and unphosphorylated forms of the AR.

To evaluate the distribution of ARs in the cells, PG-21 immunodetection was carried out in sympathetic cell culture (Figure 4B). As expected, a robust fluorescence was observed in the cell body. Moreover, a markedly punctuate distribution was also present along the axon indicating the presence of both nuclear AR and membrane AR in sympathetic neurons.

Time-lapse imaging of WGA-Alexa-546-conjugated-vesicles—To detect the movement of WGA-vesicles along the axon, we selected thin single axons; this allowed us to determine their polarity and to evaluate movement in both anterograde and retrograde direction. To quantify the WGA transport, 10 images frames/second were captured from a single axonal segment and converted into movies. We recorded time-lapse movies of 497 vesicles from 20 different experiments at 3 different time points (06hrs, 24hrs, 48hrs) each. The duration of the movies ranged from 30 to 60 sec. Table 1 summarized measurements of vesicle movements.

First, we inspected the movement of the WGA-vesicles in the axon. Consistent with *in vivo* studies, the movement of WGA-vesicles occurred in both directions (Gibson et al., 1984). Time-lapse imaging revealed a rapid movement of WGA-vesicles, which was often interrupted by prolonged pauses typical of membranous organelles (Lasek et al., 1984). For example, Figure 4D shows one WGA vesicle pausing and two moving in anterograde direction at different velocities. A few WGA-vesicles exhibited brief reversals of direction, but since these were rare and sustained for duration of less than 1 sec (and distributed equally across the three conditions), we excluded such reversal periods from the analysis.

Second, we analyzed the effect of Mibolerone on the directionality of vesicle movements. Logistic regression analysis revealed a significant conditions x time interaction ($\chi^2 = 16.4$, $p = 0.0026$) on the directionality. In particular, the effect of Mibolerone on the directionality of vesicle movements within each time points was as follows. At the first time point (06hrs), Mibolerone decreased (almost 10 fold) the ratio of anterograde to retrograde movement in both M4 and M10 conditions, relative to the control condition (Ctrl=0.2; M4=0.07; M10=0.06; Table 1); the contingency analysis of directionality showed a significant difference over the three conditions ($\chi^2 = 6.9$, $p = 0.03$). At the second time point (24 hrs), all groups increased the Antero/Retro ratio as compared with 06 hrs (Ctrl= 0.6; M4= 1; M10= 1.3), although no differences were observed across the three conditions with respect to the directionality ($\chi^2 = 2.8$, $p = 0.25$). Only the M10 treatment sustained a high Antero/Retro ratio of movement at 48 hrs (Ctrl= 0.4; M4= 0.6; M10= 1.5, $\chi^2 = 11.2$, $p = 0.004$).

Next, we calculated the effect of treatment on the longest-distance traveled (max run-length, Figure 5) by vesicles. Figure 5A show the motile behavior of three representative anterograde-moving vesicles exhibiting different run lengths. We found an increase in max run-length by anterograde-moving vesicles at 48 hrs in both M4 and M10 conditions as compared with control (Figure. 5C; M4 vs. Ctrl $p = 0.048$; M10 vs. Ctrl $p = 0.032$). The maximum run-length was higher also at 24 hrs in M10 condition as compared with M4 and control (Figure. 5B; M10 vs. M4 $p = 0.006$; M10 vs. Ctrl $p = 0.036$). The run length is a measure of the processivity of motor proteins (Thorn et al., 2000). Thus, the increased run-length observed here indicates that Mibolerone treatment is able to enhance the processivity of kinesin proteins in a dose-dependent manner. The treatment with Mibolerone at the dose of 10 nM also appeared to increase the average velocity of the anterograde movement of WGA-vesicles at both 24 and 48 hrs, as compared with 06 hours (Table 1). Unlike the above observations about the treatment- and time-related changes in anterograde transport, the number of vesicles moving in a retrograde direction, their max run-length and average velocity, were remarkably homogeneous across the three treatment conditions at each time point, suggesting that androgens regulate the efficiency of axonal transport only in the anterograde direction (Table 1).

Axon diameter—Since axonal transport plays an important role in regulating axon diameter (Eyer and Peterson, 1994; Xia et al., 2003), we measured axon diameter of the sympathetic neurons after 48h of treatment in presence of either ethanol (Ctrl) or Mibolerone at 4nM and 10nM. The quantitative morphometry of about 2000 cross-section area, revealed a significant increase of axon diameter in M10 condition as compared with Ctrl. (Ctrl, 237 ± 28.67 ; M10, 273 ± 26.88 , $n=7$ per group, $p=0.03$, percent difference = 14.12%, $d=1.28$; Figure 4C). Treatment with Mibolerone at 4nM did not affect the axonal caliber. This is not surprising given that this dose increased the efficiency of WGA axonal transport (max run length) only after 48 hrs, with no effect on the mean velocity and Antero/Retro ratio. Only the high dose (10 nm) increased the run length at 24 hrs, and the mean velocity and the Antero/Retro ratio of movement at 48 hrs. The effect on axon radial growth observed with the 10-nm dose of Mibolerone suggests that, at least in sympathetic neurons, androgens influence the axonal radial growth without being aromatized to estrogen.

Axon diameter distribution—Lastly, we evaluated the distribution of axons in the three conditions. The distributions of axon diameters for the three conditions essentially superimpose (Fig. 4). They all peak near 250 nm and all have similar skew (Ctrl= 2.45; M4= 2.34 and M10= 3.32)

Discussion

Mechanisms underlying sexual dimorphism in the maturation of WM are of considerable interest because of sex-specific vulnerabilities to psychopathology during adolescence. As demonstrated in our previous studies in humans, WM sexual dimorphisms become more prominent during adolescence under the influence of testosterone (Perrin et al., 2008, 2009).

Given this dependence of WM maturation on levels of bioavailable testosterone, here we sought to understand how this difference is sustained at the microstructural level. We use the electron microscopy to measure the diameter of myelinated and unmyelinated axons, and g ratio of myelinated axons in the splenium of intact male and female rats, and after real or sham castration carried out after weaning. Our results revealed a sex difference in myelinated axonal diameter in early adulthood (M>F; Cohen's $d = 2.7$). We also found a sex difference in g ratio (M>F; $d = 3.7$). Furthermore, removal of endogenous T by castration before puberty was associated with lower myelinated axon diameter and g ratio, as compared with intact males ($d = 1.84$ for axon diameter and $d = 2.0$ for g ratio).

To our knowledge, these observations are the first to show sex differences in the diameter and g ratio of myelinated axons. Previous studies have not reported such sex differences in the diameter of myelinated axons in young adult rats (Kim and Juraska, 1997; Kim et al., 1996). A possible reason for this discrepancy could be the strategy used to measure axon diameter. In the previous studies, the average axon diameter was estimated by measuring only the shortest diameter of each axon (in ~ 600 axons per animal). But measuring the actual diameter may not provide accurate estimates of axonal size because axons are not precisely circular. For this reason, we measured automatically the cross-sectional area of each axon and then calculated the diameter of the equivalent circle; we have done so in about 1,000 axons per animal. The relative power of our study, and the replication of these sex differences in Experiment 2, gives us some confidence in the validity of our findings. An alternative explanation may lie in the different age of rats examined. Kim and Juraska analyzed sex differences at 60 days of age, whereas we used 70 days old rats. Normally, testosterone levels rise gradually from postnatal day (PND) 20 to 40, and abruptly double by PND 50 (Matsumoto et al., 1986; Monosson et al., 1999), with a peak of testosterone concentration occurring around 50–60 days of age (Ojeada and Urbansky 1994). It is therefore possible that in these studies, animals have been analyzed before the maximal effect of testosterone on the organization of neural circuits took place. Androgens are produced in testis and adrenals; moreover, they could be also synthesized de novo in the brain (Baulieu, 1998). In the present study, we did not analyze changes on androgens levels after castration. In a previous study, others have demonstrated that gonadectomy is able to decrease considerably the levels of testosterone and its metabolite, dihydrotestosterone, both in plasma and the central nervous system when compared with the intact animals (Caruso et al., 2010).

We speculate that the thicker axons found in males reflect a role of testosterone in modulating the cellular processes underlying the radial growth of axons rather than the myelin thickness.

On surface, this finding appears inconsistent with previous results reporting a strong effect of androgens in modulating myelination (Cerghet et al., 2006; Hussain et al., 2013). But these studies estimated the amount of myelin by the number of myelinated axons, oligodendrocytes or expression of myelin proteins rather than by measuring g ratio. In our study, we evaluated the effect of testosterone on myelin volume relatively to the axonal volume. As mentioned above, g ratio increases as a function of axon diameter, indicating that the myelin thickness does not scale linearly with the axon diameter (Berthold et al., 1983; Chatzopoulou et al., 2008; Gillespie and Stein, 1983). Here, we confirm this finding and extend it by showing that the average g ratios were higher in males as compared with both females and castrated males (Figure 2A and B), further demonstrating a role of exogenous testosterone in regulating this process.

Our data do not speak to the question of possible mechanisms by which androgens regulate axon caliber. A number of possibilities exist. Androgens might affect a turnover of cytoskeletal matrix responsible for the axonal structure. In this regard, it is known that phosphorylation of both the C-terminal regions and the head domain of neurofilaments contributes to the regulation of the interactions of neurofilaments with each other, neurofilaments with microtubules, and the interactions between microtubules and motor proteins, the latter responsible for axonal transport (Julien and Mushynski, 1998). These processes may modulate the dynamics of the formation of the neurofilament-based cytoskeletal lattice supporting mature axons (Shea and Chan, 2008; Yuan et al., 2012). Androgens can modulate phosphorylation-dependent changes in protein activity by AR-dependent activation of the mitogen-activated protein kinase (MAPK/ERK) signal transduction (Nguyen et al., 2005). Androgen receptors may also exert rapid nongenomic effects through the rapid rise of intracellular calcium concentration (Ca^{2+}) (Foradori et al., 2008; Sarkey et al., 2008). Through these two distinct mechanisms, androgen can stimulate axon extension, axon branching and axonal radial growth (Estrada et al., 2006; Marron et al., 2005; Shughrue and Dorsa, 1994). It appears that androgens affect preferentially axon diameter and axon branching presumably by activation of distinct effector pathways (Lustig et al., 1994; Markus et al., 2002; Sun et al., 2003). We speculate that testosterone, by inducing neurofilament phosphorylation, can be in part responsible for the amount of neurofilaments undergoing axonal transport and in doing so, the turnover of cytoskeletal matrix responsible for the axonal radial growth. Furthermore, phosphorylation of neurofilaments is also upregulated by signals originating from myelin (Nixon et al., 1994; Sánchez et al., 2000; Starr et al., 1996); this may be one of the mechanisms responsible for the expansion of axonal diameter during development. But our *in vitro* results suggest that the presence of myelin is not necessary for androgen-related axonal growth. Thus, the higher diameter of axons found in cultured sympathetic neurons treated with the non-aromatizable Mibolerone (vs. vehicle-treated controls) suggests that, at least *in vitro*, the effect on axonal radial growth can be modulate by androgens through direct activation of AR without the interaction with glial cells. On the other hand, the absence of androgen-related effects on the

diameter of unmyelinated axons observed in our *in vivo* experiments suggest that, in myelinated axons androgens may influence axon diameter both directly (via AR acting on cytoskeleton) and indirectly (via myelin acting on cytoskeleton).

A large body of literature also indicates a positive effect of ovarian hormones on myelin formation, synthesis of myelin protein and myelin thickness. These effects can, in turn, affect the g ratio (Baulieu and Schumacher, 2000; Crawford et al., 2010; Garcia-Segura and Melcangi, 2006; Marin-Husstege et al., 2004). Therefore we cannot exclude the possibility that estrogen-mediated increase of myelination might be in part responsible for sex difference in WM maturation during puberty.

Can the testosterone-dependent increase in axon diameter affect the axon-diameter distribution? When we compared the distribution across the three groups (M, F, M gx), the results were surprising: while males showed a skewed distribution typical for most myelinated fiber-tracts (Olivares et al. 2000; Wang et al. 2008; Perge et al. 2012), the distribution in females was fairly symmetrical. Such a skewed distribution of axon diameters has been observed previously in the corpus callosum of male monkeys (*Macaca fascicularis* and *Macaca mulatta*; Tomasi et al. 2012). In our study, removal of endogenous testosterone by castration resulted in a female-like distribution in these males. Thus, circulating testosterone appears to shape the distribution of axons with different diameter (i.e., a large-axon tail) rather than simply shifting the mean towards higher values. Since the axon diameter contributes more than the connection length to the broadening of the spectrum of conduction velocities (Caminiti et al., 2013), we speculate that the observed sex differences in the axon-diameter distributions might be reflected in the broader range of conduction velocities in males, as compared with females. Future work is necessary to elucidate further this hypothesis. Unlike what we observed *in vivo*, mibolerone did not influence the axon-diameter distributions in sympathetic neurons. Since axon-diameter distribution within nerve fascicles is influenced by the anatomical constraints, namely a fixed number of fibers in an available volume (Pajevic and Basser, 2013), it is possible that the lack of such a constraint influenced the distribution of axon diameter in neurons developing in the low-density culture.

Axon growth is a complex mechanism that requires a fine orchestration of stimuli to be adequately directed to modulate synthesis and transport of axonal structural components (Goldberg, 2003). Several lines of evidence have supported axonal transport mechanism as one of the key component of axonal radial growth (Eyer and Peterson, 1994; Hoffman, 1995, 1985; Hoffman et al., 1984; Medori et al., 1985; Xia et al., 2003). Therefore, we also sought to evaluate the possible influence of Mibolerone in regulating axonal transport. Mibolerone is a highly specific synthetic non-aromatizable androgen that, like testosterone, is a ligand of the AR (Markiewicz and Gurrpide, 1997). We decided to use a synthetic ligand for AR to exclude any possible effect mediated through the aromatization of testosterone into estradiol. We showed that AR is present in both cell bodies and axons of rat sympathetic neurons indicating that androgens can exert their effects on these cells through genomic and nongenomic pathways. We used time-lapse microscopy to quantify the effect of Mibolerone on bidirectional transport of WGA vesicles in living neurons. Detailed quantification of vesicles' behavior revealed two distinct phenomena that are presumably

mediated by nongenomic and genomic pathways, respectively: 1) We found a depression of the motion in anterograde direction at the first time point (06 hrs); and 2) The anterograde movement of vesicles increased in dose-dependent manner becoming strongly favored over the retrograde transport in cells treated with 10 nM Mibolerone at 48hrs. A possible mechanism underlying depression of axonal transport at the short timescale may involve the activation of putative membrane-associated androgen receptors (mAR), which generally induces intracellular free calcium (Ca²⁺) flux (Estrada et al., 2006). These calcium oscillations are detected by specific sensor molecules, including protein kinase C (PKC) and Ca²⁺/calmodulin-dependent protein kinase II (CaMKII), able to induce signal transduction cascade and to modulate transcription activity implicated in many cellular processes (Mellström and Naranjo, 2001; Pelley et al., 2006). Recent work in mammalian neurons suggests that changes in local Ca²⁺ concentration as well as activation of CaMKII play an important part in regulating the dissociation of kinesins from microtubule or their cargoes facilitating the proper spatial and temporal dissociation of motors from their cargos (Guillaud et al., 2008; Wang and Schwarz, 2009). We speculate that the Mibolerone-mediated activation of Ca²⁺ levels may be responsible for the depression in anterograde motion induced by Mibolerone during the first six hours after its application. Surprisingly, long-term exposure to Mibolerone (48 hrs) resulted in an opposite effect: increasing the anterograde transport over the retrograde one. We found that, at high concentration (10 nM), the percentage of vesicles moving in anterograde direction was higher by 68% and 42% as compared, respectively, with the control condition and the low concentration of Mibolerone (4 nM). Moreover, we found an increase in the travelled distance by anterograde-moving vesicles in cells treated with Mibolerone 10 nM at 24 hrs and in both 10 nM and 4 nM treatments at 48 hrs as compared with control. *In vitro* studies suggest that cargoes that are attached to multiple motor-proteins are able to move further and faster than cargoes that engaged only one motor (Derr et al., 2012; Reis et al., 2012). It is possible that the long-term exposure to Mibolerone, through the activation of classical nuclear AR, is able to increase the expression of kinesin motor proteins. This may allow recruitment of multiple kinesin motors onto a single cargo leading to increases in both the rate of anterograde transport and the length of uninterrupted anterograde movements (run length). Since the force of kinesins is stronger than the opposing force of dynein motors, a small increase in the number of kinesins will be sufficient to change the directionality of transport in favour of anterograde transport (Holzbaur and Goldman, 2010). As mentioned above, axonal transport of cytoskeletal elements, mRNA, lipids and cofactors is essential for the axon growth (Martenson et al., 1993; McQuarrie and Grafstein, 1982; Vance et al., 2000; Zhang et al., 2001). In particular, expression and transport of neurofilaments, the major cytoskeletal protein within axons (Lee and Cleveland, 1996), appear to be intrinsic determinants of axon diameter; dysregulation of these processes results in an impaired radial growth of the axon (Cleveland et al., 1991; Eyer and Peterson, 1994; Hoffman, 1995; Hoffman et al., 1984; Xia et al., 2003). Available evidence suggests that neurofilaments are transported in both anterograde and retrograde directions through direct interactions with kinesin and dynein motor proteins (Jung et al., 2005; Wagner et al., 2004). (Jung et al., 2005; Wagner et al., 2004). The dynein-dynactin complex is responsible for the retrograde (minus end-directed) motion of neurofilaments on microtubules while a number of kinesin-related proteins transport neurofilaments in the anterograde (plus end) direction (Shah et al., 2000). Kinesin-

I is one of the kinesin-family proteins involved in moving neurofilaments along the axon in anterograde direction, as suggested by studies of the kinesin-I heavy chain (KIF5A) knockout mice and analyses of the effect of kinesin-I mutation on neurofilament transport in cultured neurons (Wang and Brown, 2010; Xia et al., 2003). In addition to these classical motor proteins, microfilament-based myosin VA appears to play an important role in neurofilament transport by delivering them to their microtubule tracks. This process may reduce the duration of pauses and, in turn, enhance the efficiency of neurofilament transport in axons (Alami et al., 2009). The majority of neurofilaments move in anterograde direction with a rate of movement that ranges from 0.14 to 1.4 $\mu\text{m}/\text{sec}$ (Roy et al., 2000; Wang and Brown, 2001); an inactivation of anterograde motor proteins (kinesins) results in deficit in axonal transport of neurofilaments and a reduced number of large caliber (sensory) axons (Xia et al., 2003). On the other hand, phosphorylation of neurofilaments may decrease their association with kinesin (Yabe et al., 2000, 1999), thus resulting in the accumulation of neurofilaments and subsequent radial growth of the axon (Nixon et al., 1994; Sánchez et al., 2000). The above observations suggest a role of kinesin-mediated transport of neurofilaments in regulating axonal radial growth. While the present study does not address molecular mechanisms underlying the action of testosterone on axon diameter, our findings suggest that the larger diameter found in males compared with both females and castrated males, as well as the bigger diameter found in sympathetic neuron treated with Mibolerone 10 nM, could be in part a result of the modulatory effect of testosterone on the expression levels of motor proteins and dynamics of cytoskeletal components. Further studies will be necessary to examine this possibility.

It is worth remembering that AR expression varies among distinct neuronal population of the brain with different patterns of expression through the postnatal development period in males and females. This specific context may determine selective susceptibility of specific neuronal populations to androgen actions resulting in a differential impact on axonal transport (Fernández-Guasti et al., 2000; Ravizza et al., 2002; Sheng et al., 2004). In addition, based on the relative ratio of the putative membrane AR and the classical nuclear AR, androgens may result in different effects, regulating the axon transport via distinct and potentially competing signaling pathways.

Overall, these findings support our previous hypothesis of a role of testosterone in regulating axon biology. In particular, testosterone seems to exert its effects at two levels: (1) structural - modulating the cellular processes that affect cytoskeleton and, in turn, radial growth of the axon; (2) molecular - modulating the directionality of axon transport in a time- and dose-dependent manner. The latter phenomenon – especially the rapid switch between testosterone -induced suppression and enhancement of anterograde transport - might represent a mechanism underlying some of the known effects of androgens on behavior and mental health during puberty (Patton and Viner, 2007).

Acknowledgments

This work was funded by the National Institutes of Health (5R01MH085772). We acknowledge the excellent technical assistance with electron microscopy of Mr. Battista Calvieri and Mr. Steven Doyle from the University of Toronto's Microscopy Imaging Laboratory. We also thank Celine Bourdon, Yimiao Ou and Mei Huang for advice, technical assistance and help with various experimental procedures.

References

- Alami NH, Jung P, Brown A. Myosin Va increases the efficiency of neurofilament transport by decreasing the duration of long-term pauses. *J Neurosci.* 2009; 29:6625–34.10.1523/JNEUROSCI.3829-08.2009 [PubMed: 19458233]
- Barazany D, Bassar PJ, Assaf Y. In vivo measurement of axon diameter distribution in the corpus callosum of rat brain. *Brain.* 2009; 132:1210–20.10.1093/brain/awp042 [PubMed: 19403788]
- Barry DM, Carpenter C, Yager C, Golik B, Barry KJ, Shen H, Mikse O, Eggert LS, Schulz DJ, Garcia ML. Variation of the neurofilament medium KSP repeat sub-domain across mammalian species: implications for altering axonal structure. *J Exp Biol.* 2010; 213:128–36.10.1242/jeb.033787 [PubMed: 20008369]
- Baulieu E, Schumacher M. Progesterone as a neuroactive neurosteroid, with special reference to the effect of progesterone on myelination. *Steroids.* 2000; 65:605–12. [PubMed: 11108866]
- Baulieu EE. Neurosteroids: a novel function of the brain. *Psychoneuroendocrinology.* 1998; 23:963–87. [PubMed: 9924747]
- Berthold CH, Nilsson I, Rydmark M. Axon diameter and myelin sheath thickness in nerve fibres of the ventral spinal root of the seventh lumbar nerve of the adult and developing cat. *J Anat.* 1983; 136:483–508. [PubMed: 6885614]
- Caminiti R, Carducci F, Piervincenzi C, Battaglia-Mayer A, Confalone G, Visco-Comandini F, Pantano P, Innocenti GM. Diameter, length, speed, and conduction delay of callosal axons in macaque monkeys and humans: comparing data from histology and magnetic resonance imaging diffusion tractography. *J Neurosci.* 2013; 33:14501–11.10.1523/JNEUROSCI.0761-13.2013 [PubMed: 24005301]
- Caruso D, Pesaresi M, Maschi O, Giatti S, Garcia-Segura LM, Melcangi RC. Effect of short-and long-term gonadectomy on neuroactive steroid levels in the central and peripheral nervous system of male and female rats. *J Neuroendocrinol.* 2010; 22:1137–47.10.1111/j.1365-2826.2010.02064.x [PubMed: 20819120]
- Cerghet M, Skoff RP, Bessert D, Zhang Z, Mullins C, Ghandour MS. Proliferation and death of oligodendrocytes and myelin proteins are differentially regulated in male and female rodents. *J Neurosci.* 2006; 26:1439–47.10.1523/JNEUROSCI.2219-05.2006 [PubMed: 16452667]
- Chatzopoulou E, Miguez A, Savvaki M, Levasseur G, Muzerelle A, Muriel MP, Goureau O, Watanabe K, Goutebroze L, Gaspar P, Zalc B, Karageorgos D, Thomas JL. Structural requirement of TAG-1 for retinal ganglion cell axons and myelin in the mouse optic nerve. *J Neurosci.* 2008; 28:7624–36.10.1523/JNEUROSCI.1103-08.2008 [PubMed: 18650339]
- Ciccolini F, Collins TJ, Sudhoelter J, Lipp P, Berridge MJ, Bootman MD. Local and global spontaneous calcium events regulate neurite outgrowth and onset of GABAergic phenotype during neural precursor differentiation. *J Neurosci.* 2003; 23:103–11. [PubMed: 12514206]
- Cleveland DW, Monteiro MJ, Wong PC, Gill SR, Gearhart JD, Hoffman PN. Involvement of neurofilaments in the radial growth of axons. *J Cell Sci Suppl.* 1991; 15:85–95. [PubMed: 1824110]
- Colin E, Zala D, Liot G, Rangone H, Borrell-Pagès M, Li XJ, Saudou F, Humbert S. Huntingtin phosphorylation acts as a molecular switch for anterograde/retrograde transport in neurons. *EMBO J.* 2008; 27:2124–34.10.1038/emboj.2008.133 [PubMed: 18615096]
- Crawford DK, Mangiardi M, Song B, Patel R, Du S, Sofroniew MV, Voskuhl RR, Tiwari-Woodruff SK. Oestrogen receptor beta ligand: a novel treatment to enhance endogenous functional remyelination. *Brain.* 2010; 133:2999–3016.10.1093/brain/awq237 [PubMed: 20858739]
- Derr ND, Goodman BS, Jungmann R, Leschziner AE, Shih WM, Reck-Peterson SL. Tug-of-war in motor protein ensembles revealed with a programmable DNA origami scaffold. *Science.* 2012; 338:662–5.10.1126/science.1226734 [PubMed: 23065903]
- DonCarlos LL, Sarkey S, Lorenz B, Azcoitia I, Garcia-Ovejero D, Huppenbauer C, Garcia-Segura LM. Novel cellular phenotypes and subcellular sites for androgen action in the forebrain. *Neuroscience.* 2006; 138:801–7.10.1016/j.neuroscience.2005.06.020 [PubMed: 16310968]
- Durdiakova J, Ostatnikova D, Celec P. Testosterone and its metabolites--modulators of brain functions. *Acta Neurobiol Exp (Wars).* 2011; 71:434–54. [PubMed: 22237492]

- Estrada M, Uhlen P, Ehrlich BE. Ca²⁺ oscillations induced by testosterone enhance neurite outgrowth. *J Cell Sci.* 2006; 119:733–43.10.1242/jcs.02775 [PubMed: 16449326]
- Eyer J, Peterson A. Neurofilament-deficient axons and perikaryal aggregates in viable transgenic mice expressing a neurofilament-beta-galactosidase fusion protein. *Neuron.* 1994; 12:389–405. [PubMed: 8110465]
- Fernández-Guasti A, Kruijver FP, Fodor M, Swaab DF. Sex differences in the distribution of androgen receptors in the human hypothalamus. *J Comp Neurol.* 2000; 425:422–35. [PubMed: 10972942]
- Foradori C, Weiser M, Handa R. Non-genomic actions of androgens. *Front Neuroendocrinol.* 2008; 29:169–181.10.1016/j.yfme.2007.10.005.Non-genomic [PubMed: 18093638]
- Garcia-Segura LM, Melcangi RC. Steroids and glial cell function. *Glia.* 2006; 54:485–98.10.1002/glia.20404 [PubMed: 16906540]
- Gatson JW, Singh M. Activation of a membrane-associated androgen receptor promotes cell death in primary cortical astrocytes. *Endocrinology.* 2007; 148:2458–64.10.1210/en.2006-1443 [PubMed: 17303658]
- Gibson AR, Hansma DI, Houk JC, Robinson FR. A sensitive low artifact TMB procedure for the demonstration of WGA-HRP in the CNS. *Brain Res.* 1984; 298:235–41. [PubMed: 6202368]
- Gillespie MJ, Stein RB. The relationship between axon diameter, myelin thickness and conduction velocity during atrophy of mammalian peripheral nerves. *Brain Res.* 1983; 259:41–56. [PubMed: 6824935]
- Goldberg JL. How does an axon grow? *Genes Dev.* 2003; 17:941–58.10.1101/gad.1062303 [PubMed: 12704078]
- Guillaud L, Wong R, Hirokawa N. Disruption of KIF17-Mint1 interaction by CaMKII-dependent phosphorylation: a molecular model of kinesin-cargo release. *Nat Cell Biol.* 2008; 10:19–29.10.1038/ncb1665 [PubMed: 18066053]
- Herting MM, Maxwell EC, Irvine C, Nagel BJ. The impact of sex, puberty, and hormones on white matter microstructure in adolescents. *Cereb Cortex.* 2012; 22:1979–92.10.1093/cercor/bhr246 [PubMed: 22002939]
- Hirokawa N, Niwa S, Tanaka Y. Molecular motors in neurons: transport mechanisms and roles in brain function, development, and disease. *Neuron.* 2010; 68:610–38.10.1016/j.neuron.2010.09.039 [PubMed: 21092854]
- Hoffman PN. Changes in neurofilament transport coincide temporally with alterations in the caliber of axons in regenerating motor fibers. *J Cell Biol.* 1985; 101:1332–1340.10.1083/jcb.101.4.1332 [PubMed: 2413041]
- Hoffman PN. Review: The Synthesis, Axonal Transport, and Phosphorylation of Neurofilaments Determine Axonal Caliber in Myelinated Nerve Fibers. *Neurosci.* 1995; 1:76–83.10.1177/107385849500100204
- Hoffman PN, Griffin JW, Price DL. Control of axonal caliber by neurofilament transport. *J Cell Biol.* 1984; 99:705–14. [PubMed: 6204997]
- Holzbaur ELF, Goldman YE. Coordination of molecular motors: from in vitro assays to intracellular dynamics. *Curr Opin Cell Biol.* 2010; 22:4–13.10.1016/j.ceb.2009.12.014 [PubMed: 20102789]
- Hussain R, Ghomari AM, Bielecki B, Steibel J, Boehm N, Liere P, Macklin WB, Kumar N, Habert R, Mhaouty-Kodja S, Tronche F, Sitruk-Ware R, Schumacher M, Ghandour MS. The neural androgen receptor: a therapeutic target for myelin repair in chronic demyelination. *Brain.* 2013; 136:132–46.10.1093/brain/aws284 [PubMed: 23365095]
- Julien JP, Mushynski WE. Neurofilaments in health and disease. *Prog Nucleic Acid Res Mol Biol.* 1998; 61:1–23. [PubMed: 9752717]
- Jung C, Lee S, Ortiz D, Zhu Q, Julien JP, Shea TB. The high and middle molecular weight neurofilament subunits regulate the association of neurofilaments with kinesin: inhibition by phosphorylation of the high molecular weight subunit. *Brain Res Mol Brain Res.* 2005; 141:151–5.10.1016/j.molbrainres.2005.08.009 [PubMed: 16246456]
- Kampa M, Papakonstanti EA, Hatzoglou A, Stathopoulos EN, Stournaras C, Castanas E. The human prostate cancer cell line LNCaP bears functional membrane testosterone receptors that increase PSA secretion and modify actin cytoskeleton. *FASEB J.* 2002; 16:1429–31.10.1096/fj.02-0131fje [PubMed: 12205037]

- Kim JH, Juraska JM. Sex differences in the development of axon number in the splenium of the rat corpus callosum from postnatal day 15 through 60. *Brain Res Dev Brain Res*. 1997; 102:77–85.
- Kim JHY, Ellman A, Juraska JM. A re-examination of sex differences in axon density and number in the splenium of the rat corpus callosum. 1996; 740:47–56.
- Lasek RJ, Garner JA, Brady ST. Axonal transport of the cytoplasmic matrix. *J Cell Biol*. 1984; 99:212s–221s. [PubMed: 6378920]
- Lee MK, Cleveland DW. Neuronal intermediate filaments. *Annu Rev Neurosci*. 1996; 19:187–217.10.1146/annurev.ne.19.030196.001155 [PubMed: 8833441]
- Lustig R, Hua P, Smith L. An in Vitro Model for the Effects of Androgen on Neurons Employing Androgen Receptor-Transfected PC12 Cells. *Mol Cell* 1994
- Marin-Husstege M, Muggironi M, Raban D, Skoff RP, Casaccia-Bonnel P. Oligodendrocyte progenitor proliferation and maturation is differentially regulated by male and female sex steroid hormones. *Dev Neurosci*. 2004; 26:245–54.10.1159/000082141 [PubMed: 15711064]
- Markiewicz L, Gurskide E. Estrogenic and progestagenic activities of physiologic and synthetic androgens, as measured by in vitro bioassays. *Methods Find Exp Clin Pharmacol*. 1997; 19:215–22. [PubMed: 9228646]
- Markus A, Zhong J, Snider WD. Raf and akt mediate distinct aspects of sensory axon growth. *Neuron*. 2002; 35:65–76. [PubMed: 12123609]
- Marron TU, Guerini V, Rusmini P, Sau D, Brevini TaL, Martini L, Poletti a. Androgen-induced neurite outgrowth is mediated by neuritin in motor neurones. *J Neurochem*. 2005; 92:10–20.10.1111/j.1471-4159.2004.02836.x [PubMed: 15606892]
- Martenson C, Stone K, Reedy M, Sheetz M. Fast axonal transport is required for growth cone advance. *Nature*. 1993; 366:66–9.10.1038/366066a0 [PubMed: 7694151]
- Matsumoto AM, Karpas AE, Southworth MB, Dorsa DM, Bremner WJ. Evidence for activation of the central nervous system-pituitary mechanism for gonadotropin secretion at the time of puberty in the male rat. *Endocrinology*. 1986; 119:362–9.10.1210/endo-119-1-362 [PubMed: 3522211]
- McQuarrie IG, Grafstein B. Protein synthesis and axonal transport in goldfish retinal ganglion cells during regeneration accelerated by a conditioning lesion. *Brain Res*. 1982; 251:25–37. [PubMed: 6184129]
- Medori R, Autilio-Gambetti L, Monaco S, Gambetti P. Experimental diabetic neuropathy: impairment of slow transport with changes in axon cross-sectional area. *Proc Natl Acad Sci U S A*. 1985; 82:7716–20. [PubMed: 2415969]
- Mellström B, Naranjo JR. Mechanisms of Ca(2+)-dependent transcription. *Curr Opin Neurobiol*. 2001; 11:312–9. [PubMed: 11399429]
- Midorikawa R, Takei Y, Hirokawa N. KIF4 motor regulates activity-dependent neuronal survival by suppressing PARP-1 enzymatic activity. *Cell*. 2006; 125:371–83.10.1016/j.cell.2006.02.039 [PubMed: 16630823]
- Monosson E, Kelce WR, Lambright C, Ostby J, Gray LE. Peripubertal exposure to the antiandrogenic fungicide, vinclozolin, delays puberty, inhibits the development of androgen-dependent tissues, and alters androgen receptor function in the male rat. *Toxicol Ind Health*. 1999; 15:65–79.10.1177/074823379901500107 [PubMed: 10188192]
- Morfini G, Szebenyi G, Elluru R, Ratner N, Brady ST. Glycogen synthase kinase 3 phosphorylates kinesin light chains and negatively regulates kinesin-based motility. *EMBO J*. 2002; 21:281–93.10.1093/emboj/21.3.281 [PubMed: 11823421]
- Murayama Y, Weber B, Saleem KS, Augath M, Logothetis NK. Tracing neural circuits in vivo with Mn-enhanced MRI. *Magn Reson Imaging*. 2006; 24:349–58.10.1016/j.mri.2005.12.031 [PubMed: 16677940]
- Nguyen T-VV, Yao M, Pike CJ. Androgens activate mitogen-activated protein kinase signaling: role in neuroprotection. *J Neurochem*. 2005; 94:1639–51.10.1111/j.1471-4159.2005.03318.x [PubMed: 16011741]
- Nixon RA, Paskevich PA, Sihag RK, Thayer CY. Phosphorylation on carboxyl terminus domains of neurofilament proteins in retinal ganglion cell neurons in vivo: influences on regional neurofilament accumulation, interneurofilament spacing, and axon caliber. *J Cell Biol*. 1994; 126:1031–46. [PubMed: 7519617]

- Olivares R, Michalland S, Aboitiz F. Cross-species and intraspecies morphometric analysis of the corpus callosum. *Brain Behav Evol.* 2000; 55:37–43. 6640. [PubMed: 10773624]
- Olivares R, Montiel J, Aboitiz F. Species differences and similarities in the fine structure of the mammalian corpus callosum. *Brain Behav Evol.* 2001; 57:98–105. 47229. [PubMed: 11435670]
- Ojeda, SR.; Urbanski, HF. Puberty in the rat. In: Knobil, E.; Neill, JD., editors. *The Physiology of Reproduction*. 2. Raven Press, Inc; New York, NY: 1994. p. 363-409.
- Pajevic S, Basser PJ. An optimum principle predicts the distribution of axon diameters in normal white matter. *PLoS One.* 2013; 8:e54095.10.1371/journal.pone.0054095 [PubMed: 23382870]
- Patton GC, Viner R. Pubertal transitions in health. *Lancet.* 2007; 369:1130–9.10.1016/S0140-6736(07)60366-3 [PubMed: 17398312]
- Paus T. Growth of white matter in the adolescent brain: myelin or axon? *Brain Cogn.* 2010; 72:26–35.10.1016/j.bandc.2009.06.002 [PubMed: 19595493]
- Paus T, Pesaresi M, French L. White matter as a transport system. *Neuroscience.* 2014.10.1016/j.neuroscience.2014.01.055
- Pelley RP, Chinnakannu K, Murthy S, Strickland FM, Menon M, Dou QP, Barrack ER, Reddy GPV. Calmodulin-androgen receptor (AR) interaction: calcium-dependent, calpain-mediated breakdown of AR in LNCaP prostate cancer cells. *Cancer Res.* 2006; 66:11754–62.10.1158/0008-5472.CAN-06-2918 [PubMed: 17178871]
- Peper JS, Hulshoff Pol HE, Crone EA, van Honk J. Sex steroids and brain structure in pubertal boys and girls: a mini-review of neuroimaging studies. *Neuroscience.* 2011; 191:28–37.10.1016/j.neuroscience.2011.02.014 [PubMed: 21335066]
- Perge, Ja; Niven, JE.; Mugnaini, E.; Balasubramanian, V.; Sterling, P. Why do axons differ in caliber? *J Neurosci.* 2012; 32:626–38.10.1523/JNEUROSCI.4254-11.2012 [PubMed: 22238098]
- Perrin JS, Hervé PY, Leonard G, Perron M, Pike GB, Pitiot A, Richer L, Veillette S, Pausova Z, Paus T. Growth of white matter in the adolescent brain: role of testosterone and androgen receptor. *J Neurosci.* 2008; 28:9519–24.10.1523/JNEUROSCI.1212-08.2008 [PubMed: 18799683]
- Perrin JS, Leonard G, Perron M, Pike GB, Pitiot a, Richer L, Veillette S, Pausova Z, Paus T. Sex differences in the growth of white matter during adolescence. *Neuroimage.* 2009; 45:1055–66.10.1016/j.neuroimage.2009.01.023 [PubMed: 19349224]
- Perrot R, Julien JP. Real-time imaging reveals defects of fast axonal transport induced by disorganization of intermediate filaments. *FASEB J.* 2009; 23:3213–25.10.1096/fj.09-129585 [PubMed: 19451279]
- Peters, A.; Palay, SL.; de Webster, HF. *Fine Structure of the Nervous System: Neurons and Their Supporting Cells.* Oxford University Press; USA: 1991.
- Ravizza T, Galanopoulou AS, Velísková J, Moshé SL. Sex differences in androgen and estrogen receptor expression in rat substantia nigra during development: an immunohistochemical study. *Neuroscience.* 2002; 115:685–96. [PubMed: 12435407]
- Reis GF, Yang G, Szpankowski L, Weaver C, Shah SB, Robinson JT, Hays TS, Danuser G, Goldstein LSB. Molecular motor function in axonal transport in vivo probed by genetic and computational analysis in *Drosophila*. *Mol Biol Cell.* 2012; 23:1700–14.10.1091/mbc.E11-11-0938 [PubMed: 22398725]
- Roy S, Coffee P, Smith G, Liem RK, Brady ST, Black MM. Neurofilaments are transported rapidly but intermittently in axons: implications for slow axonal transport. *J Neurosci.* 2000; 20:6849–6861. [pii]. [PubMed: 10995829]
- Sánchez I, Hassinger L, Sihag RK, Cleveland DW, Mohan P, Nixon Ra. Local control of neurofilament accumulation during radial growth of myelinating axons in vivo. Selective role of site-specific phosphorylation. *J Cell Biol.* 2000; 151:1013–24. [PubMed: 11086003]
- Sarkey S, Azcoitia I, Garcia-Segura LM, Garcia-Ovejero D, DonCarlos LL. Classical androgen receptors in non-classical sites in the brain. *Horm Behav.* 2008; 53:753–64.10.1016/j.yhbeh.2008.02.015 [PubMed: 18402960]
- Sato N, Sadar MD, Bruchoovsky N, Saatcioglu F, Rennie PS, Sato S, Lange PH, Gleave ME. Androgenic induction of prostate-specific antigen gene is repressed by protein-protein interaction between the androgen receptor and AP-1/c-Jun in the human prostate cancer cell line LNCaP. *J Biol Chem.* 1997; 272:17485–94. [PubMed: 9211894]

- Schwab ME, Suda K, Thoenen H. Selective retrograde transsynaptic transfer of a protein, tetanus toxin, subsequent to its retrograde axonal transport. *J Cell Biol.* 1979; 82:798–810. [PubMed: 92475]
- Shah JV, Flanagan LA, Janmey PA, Leterrier JF. Bidirectional translocation of neurofilaments along microtubules mediated in part by dynein/dynactin. *Mol Biol Cell.* 2000; 11:3495–508. [PubMed: 11029051]
- Shea TB, Chan WKH. Regulation of neurofilament dynamics by phosphorylation. *Eur J Neurosci.* 2008; 27:1893–901.10.1111/j.1460-9568.2008.06165.x [PubMed: 18412610]
- Sheng Z, Kawano J, Yanai A, Fujinaga R, Tanaka M, Watanabe Y, Shinoda K. Expression of estrogen receptors (alpha, beta) and androgen receptor in serotonin neurons of the rat and mouse dorsal raphe nuclei; sex and species differences. *Neurosci Res.* 2004; 49:185–96.10.1016/j.neures.2004.02.011 [PubMed: 15140561]
- Shughrue PJ, Dorsa DM. Estrogen and androgen differentially modulate the growth-associated protein GAP-43 (neuromodulin) messenger ribonucleic acid in postnatal rat brain. *Endocrinology.* 1994; 134:1321–8. [PubMed: 8119173]
- Simerly RB, Chang C, Muramatsu M, Swanson LW. Distribution of androgen and estrogen receptor mRNA-containing cells in the rat brain: an in situ hybridization study. *J Comp Neurol.* 1990; 294:76–95.10.1002/cne.902940107 [PubMed: 2324335]
- Starr R, Attema B, DeVries GH, Monteiro MJ. Neurofilament phosphorylation is modulated by myelination. *J Neurosci Res.* 1996; 44:328–37.10.1002/(SICI)1097-4547(19960515)44:4<328::AID-JNR3>3.0.CO;2-E [PubMed: 8739151]
- Steinsapir J, Socci R, Reinach P. Effects of androgen on intracellular calcium of LNCaP cells. *Biochem Biophys Res Commun.* 1991; 179:90–6. [PubMed: 1883394]
- Sun M, Yang L, Feldman RI, Sun XM, Bhalla KN, Jove R, Nicosia SV, Cheng JQ. Activation of phosphatidylinositol 3-kinase/Akt pathway by androgen through interaction of p85 α , androgen receptor, and Src. *J Biol Chem.* 2003; 278:42992–43000. [PubMed: 12933816]
- Thorn KS, Ubersax JA, Vale RD. Engineering the processive run length of the kinesin motor. *J Cell Biol.* 2000; 151:1093–100. [PubMed: 11086010]
- Tomasi S, Caminiti R, Innocenti GM. Areal differences in diameter and length of corticofugal projections. *Cereb Cortex.* 2012; 22:1463–72.10.1093/cercor/bhs011 [PubMed: 22302056]
- Ullén F. Is activity regulation of late myelination a plastic mechanism in the human nervous system? *Neuron Glia Biol.* 2009; 5:29–34.10.1017/S1740925X09990330 [PubMed: 19785923]
- Vaillant AR, Mazzoni I, Tudan C, Boudreau M, Kaplan DR, Miller FD. Depolarization and neurotrophins converge on the phosphatidylinositol 3-kinase-Akt pathway to synergistically regulate neuronal survival. *J Cell Biol.* 1999; 146:955–66. [PubMed: 10477751]
- Vaillant AR, Zanassi P, Walsh GS, Aumont A, Alonso A, Miller FD. Signaling mechanisms underlying reversible, activity-dependent dendrite formation. *Neuron.* 2002; 34:985–98. [PubMed: 12086645]
- Vance JE, Campenot RB, Vance DE. The synthesis and transport of lipids for axonal growth and nerve regeneration. *Biochim Biophys Acta.* 2000; 1486:84–96. [PubMed: 10856715]
- Wagner OI, Ascaño J, Tokito M, Leterrier JF, Janmey PA, Holzbaur ELF. The interaction of neurofilaments with the microtubule motor cytoplasmic dynein. *Mol Biol Cell.* 2004; 15:5092–100.10.1091/mbc.E04-05-0401 [PubMed: 15342782]
- Wang L, Brown a. Rapid intermittent movement of axonal neurofilaments observed by fluorescence photobleaching. *Mol Biol Cell.* 2001; 12:3257–67. [PubMed: 11598207]
- Wang L, Brown A. Rapid movement of microtubules in axons. *Curr Biol.* 2002; 12:1496–1501. [PubMed: 12225664]
- Wang L, Brown A. A hereditary spastic paraplegia mutation in kinesin-1A/KIF5A disrupts neurofilament transport. *Mol Neurodegener.* 2010; 5:52.10.1186/1750-1326-5-52 [PubMed: 21087519]
- Wang SSH, Shultz JR, Burish MJ, Harrison KH, Hof PR, Towns LC, Wagers MW, Wyatt KD. Functional trade-offs in white matter axonal scaling. *J Neurosci.* 2008; 28:4047–56.10.1523/JNEUROSCI.5559-05.2008 [PubMed: 18400904]

- Wang X, Schwarz TL. The mechanism of Ca²⁺-dependent regulation of kinesin-mediated mitochondrial motility. *Cell*. 2009; 136:163–74.10.1016/j.cell.2008.11.046 [PubMed: 19135897]
- Xia C-H, Roberts EA, Her L-S, Liu X, Williams DS, Cleveland DW, Goldstein LSB. Abnormal neurofilament transport caused by targeted disruption of neuronal kinesin heavy chain KIF5A. *J Cell Biol*. 2003; 161:55–66.10.1083/jcb.200301026 [PubMed: 12682084]
- Yabe JT, Jung C, Chan WK, Shea TB. Phospho-dependent association of neurofilament proteins with kinesin in situ. *Cell Motil Cytoskeleton*. 2000; 45:249–62.10.1002/(SICI)1097-0169(200004)45:4<249::AID-CM1>3.0.CO;2-M [PubMed: 10744858]
- Yabe JT, Pimenta A, Shea TB. Kinesin-mediated transport of neurofilament protein oligomers in growing axons. *J Cell Sci*. 1999; 112(Pt 2):3799–814. [PubMed: 10523515]
- Yuan A, Rao MV, Veeranna, Nixon Ra. Neurofilaments at a glance. *J Cell Sci*. 2012; 125:3257–63.10.1242/jcs.104729 [PubMed: 22956720]
- Zhang HL, Eom T, Oleynikov Y, Shenoy SM, Liebelt DA, Dictenberg JB, Singer RH, Bassell GJ. Neurotrophin-induced transport of a beta-actin mRNP complex increases beta-actin levels and stimulates growth cone motility. *Neuron*. 2001; 31:261–75. [PubMed: 11502257]

Highlights

- In humans, volume and properties of white matter change during male adolescence
- Here we show that axons are thicker in male than female rats
- Castration at weaning eliminates this structural sex difference
- Synthetic testosterone affects axonal transport in vitro

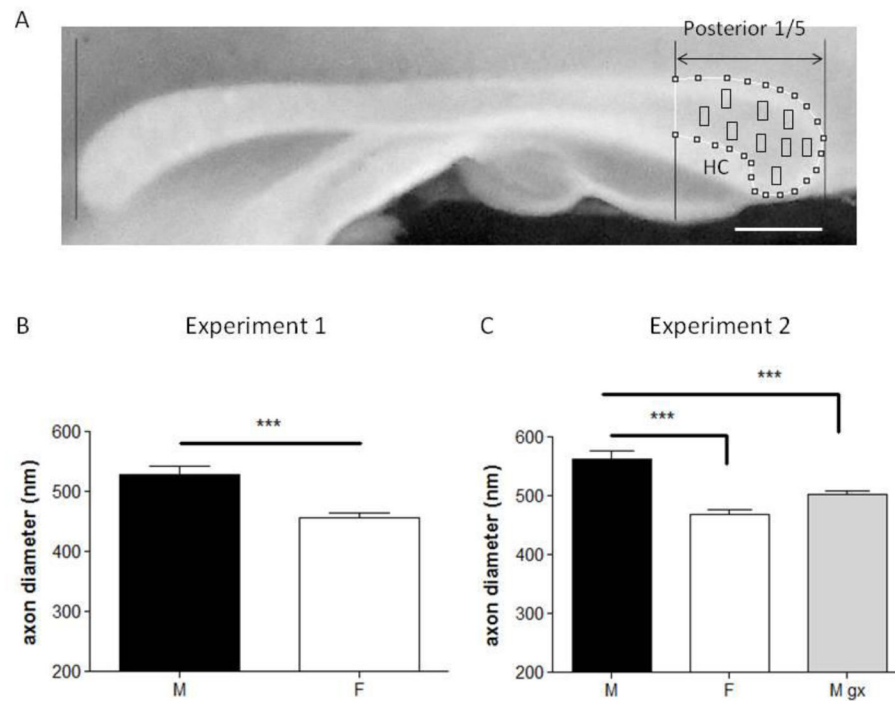


Figure 1.

A, Representative digital image of the rat corpus callosum in a midsagittal section. Rostral is to the left. The lines at the two edges were used to delineate the splenium. Axon diameter was assessed within the area delimited by the black rectangles. HC denotes dorsal hippocampal commissure. Scale bars, 1 mm.

B and C, Barplots showing the results of axon diameter in Experiment 1 and 2 respectively. C, Mean axon diameter of myelinated axons was greater in males compared with females. Gonadectomized males showed a significant decrease in the axon diameter as compared with intact males. *** $p < 0.001$ vs. males. M = males; F = females; M gx = males gonadectomised.

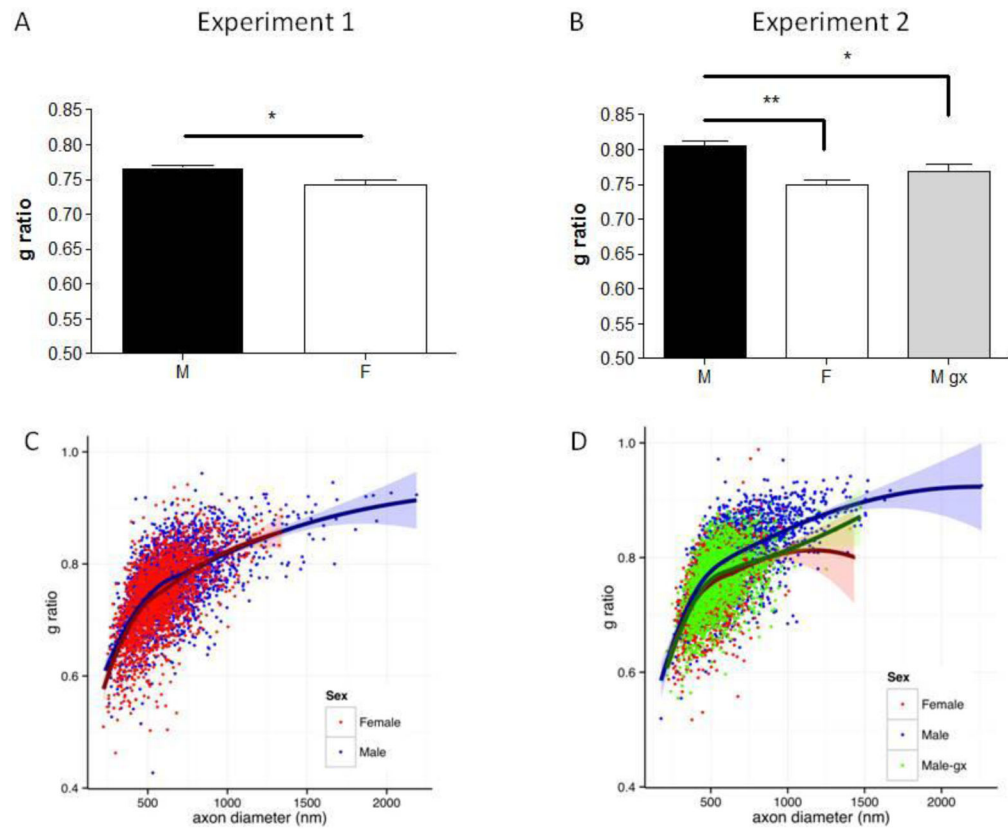


Figure 2.

A and B, Barplots showing the results of g ratio quantification in Experiment 1 and 2 respectively. The median values of g ratio from individual animals were used for analysis of variance. g ratio calculated in intact male and females was higher in males, as compared with females. Removal of endogenous T decreased g ratio in gonadectomized males to values similar to females. ** $p < 0.01$ vs. Males; * $p < 0.05$ vs. Males. M = males; F = females; M gx = males gonadectomised.

C, Scatter plot of g ratio and axon diameter. The plot represents the grouped data from all axons of Experiment 1 in intact males (blue) and intact females (red). A Local Polynomial Regression curve (LOESS) is shown for each sex, with 95% confidence intervals as shaded bands.

D, Scatter plot of g ratio and axon diameter. The plot represents the grouped data from all axons of Experiment 2 in intact males (blue), gonadectomized males (green) and intact females (red). A Local Polynomial Regression curve (LOESS) is shown for each sex, with 95% confidence intervals as shaded bands. In both experiments, the average g ratio obtained in intact males appears to differ from both females and M gx for axons with diameters in the range of 400–800 nm. As can be seen from the plots, this range contains the majority of axons.

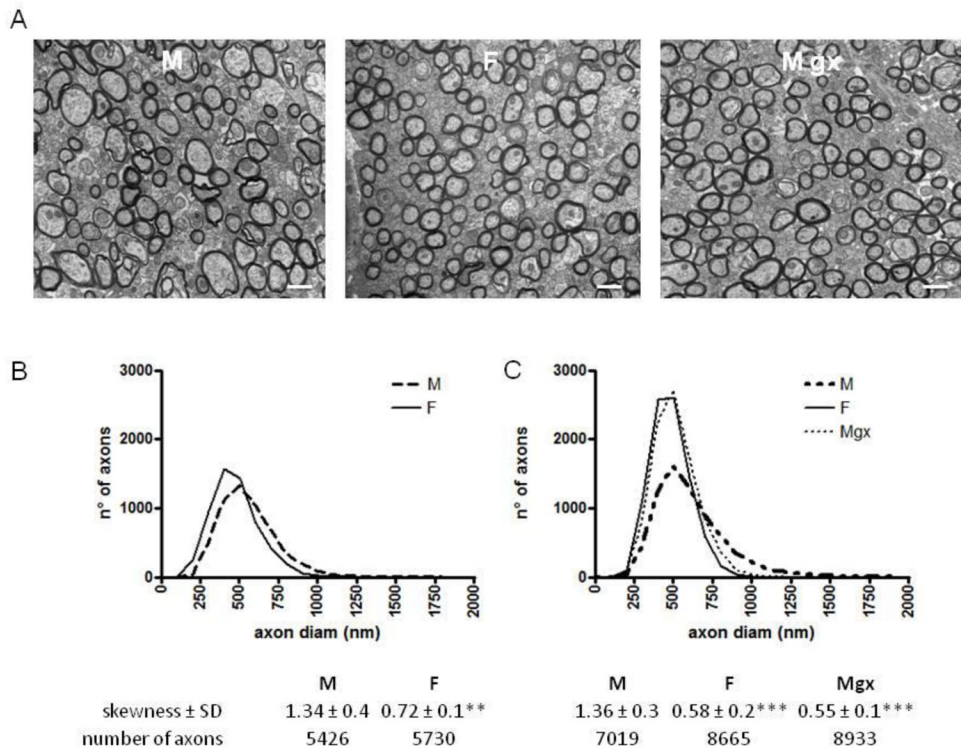


Figure 3.

A, Electron micrographs showing representative myelinated axons in cross sections of splenium of corpus callosum in an intact male, intact female and gonadectomized male rat. B and C, Distribution of fiber diameters in Experiment 1 and Experiment 2. The distribution in intact males is broader, with a strong skew. Intact females and gonadectomized males show fairly symmetrical distribution, with a small skew. *** $p < 0.001$ vs. males; ** $p < 0.01$ vs. males. M = males; F = females; M gx = males gonadectomized. Scale bars, 500 μ m.

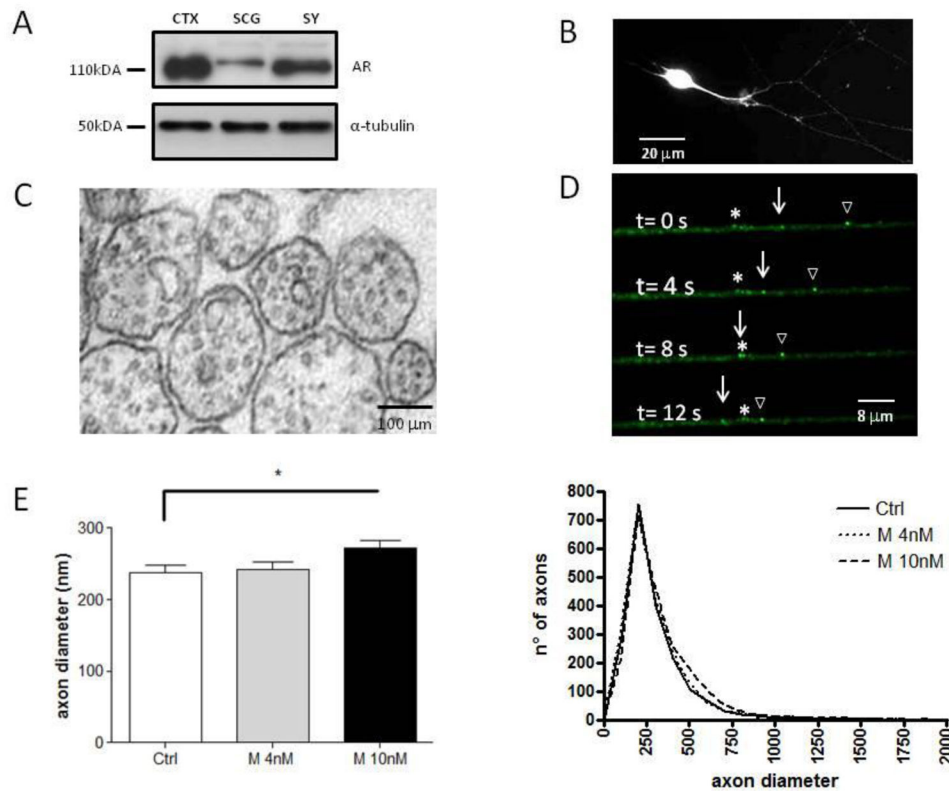


Figure 4.

A, Western blot showing expression of AR. Homogenates of superior cervical ganglion and sympathetic cell culture lysate show a band of the expected molecular weight for the AR protein (110 kDa), which coincides with the control band of brain cortex homogenate. α -tubulin was used as a loading control. CTX, cortex; SCG, superior cervical ganglion; Sy, sympathetic neurons.

B, Immunostaining for the AR epitope reveals AR expression throughout cell bodies and neurites. AR is homogeneously distributed in the cell body, and in a punctate pattern along the processes of sympathetic neurons. Scale bar = 20 μ m.

C, Electron micrographs showing representative axonal cross-section from sympathetic neurons. Abundant round microtubules are visible as well as membranous organelles.

D, Example of WGA vesicles moving in anterograde direction, empty triangle sign and white arrow. Asterisk indicates a stationary WGA vesicle. The images shown here were selected from a time-lapse movie in which images were acquired at 10 images frames/second.

E, Barplots showing the results of axon diameter quantification in sympathetic neurons. Mean axon diameter of myelinated axons was greater in Mibolerone 10nM (n = 2065 axons) as compared with Control (n = 1915 axons) but not with Mibolerone 4nM (n = 1979 axons). *p < 0.05 vs. Mibolerone 10nM.

F, Distribution of fiber diameters in sympathetic cell culture. All three conditions show similar distribution of diameters. Ctrl = Control; M 4nM = Mibolerone 4nM; M 10nM = Mibolerone 10nM.

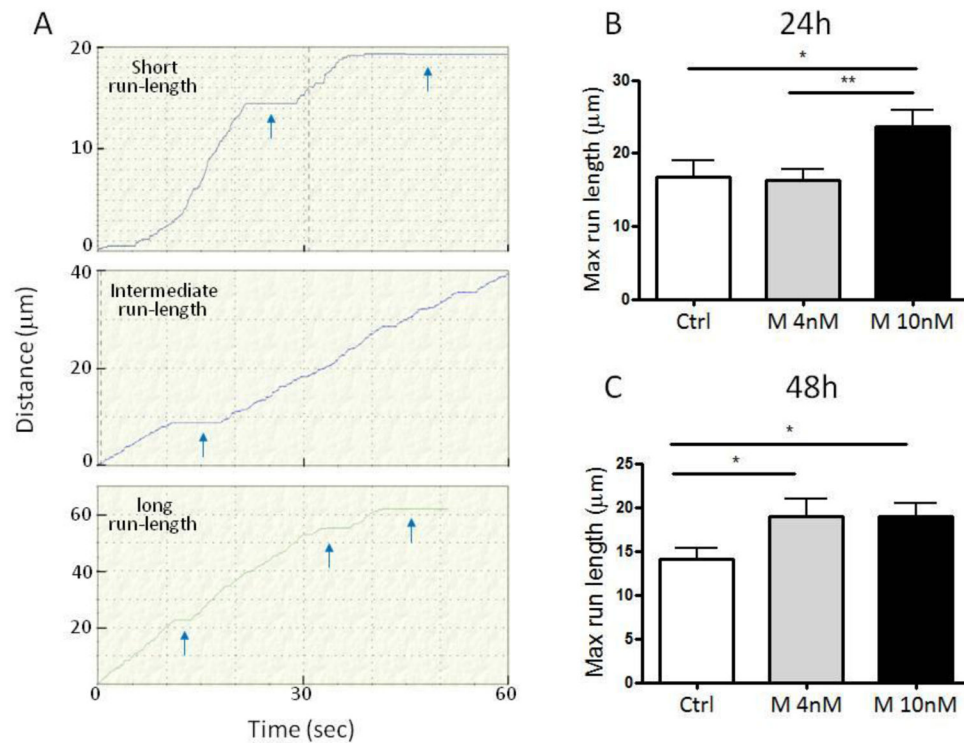


Figure 5.

A, Graphical representation of anterograde movement of three representative vesicles at 48 hrs. The Y-axis represent the distance of the vesicle from its initial location. The X-axis represents the time of the movie. In some cases the acquisition interval was less than 60 sec because the vesicle move outside of the imaged region.

B, Barplot of average max run-length (the longest distance traveled by vesicles between two pauses) in anterograde direction at 24 hrs. Control (n = 18); Mibolerone 4nM (n = 26); Mibolerone 10nM (n = 28). **p < 0.01 vs. Mibolerone 10nM; *p < 0.05 vs. Mibolerone 10nM.

C, Barplot of average max run-length in anterograde direction at 48 hrs. Ctrl (n = 16); Mibolerone 4nM (n = 17); Mibolerone 10nM (n = 35). *p < 0.05 vs. Mibolerone 10nM. Ctrl = Control; M 4nM = Mibolerone 4nM; M 10nM = Mibolerone 10nM.

Table 1

Direction	Ctrl			M4			M10				
	06h	24h	48h	0000	06h	24h	48h	0000	06h	24h	48h
<i>Anterograde</i>											
Number vesicles	13	18	16	3	26	17	4	28	35		
In Motion (%)	51	70	58	51	69	70	45	79	69		
Max run length (µm)	14.5±9.7	16.8±9.0	14.1±4.8	18.9±6.5	16.36±6.9	18.9±8.2#	19.53±26	23.7±11##	18.6±8.3#		
Average velocity (µ/sec)	1±0.9	1.5±0.6	1.3±0.5	0.6±0.1	1.5±0.7	1.5±0.6	0.4±0.6	1.6±0.6***	1.4±0.5**		
Peak velocity (µ/sec)	1.4±1.2	1.8±0.7	1.7±0.7	0.7±0.2	1.9±0.6	1.9±0.6	1.0±0.3	1.9±0.6	1.7±0.7		
<i>Retrograde</i>											
Number vesicles	60	27	38	46	26	26	66	21	23		
In Motion (%)	53	55	59	56	55	60	52	21	23		
Max run length (µm)	12.7±6.9	13.4±7.3	14.5±8.1	12.9±8.1	12.2±6.1	16.1±9.7	14.4±10.5	15.0±10	15.5±9.7		
Average velocity (µ/sec)	0.8±0.4	0.9±0.3	0.8±0.4	0.7±0.2	0.7±0.2	0.7±0.3	0.8±0.4	0.9±0.3	0.9±0.4		
Peak velocity (µ/sec)	1.2±0.8	1.3±0.4	1.1±0.4	1.1±0.5	1.0±0.3	1.0±0.4	1.1±0.6	1.2±0.3	1.2±0.6		
Antero/Retro	0.2	0.6	0.4	0.07	1	0.6	0.06	1.3	1.5		

*** p<0.001 vs. 06h within the same condition;

** p<0.01 vs. 06h within the same condition

p<0.01 vs. Ctrl within the same time point;

p<0.05 vs. Ctrl within the same time point